PROBABILISTIC ANALYSIS AND FINITE ELEMENT MODELING OF INFINITE SLOPES

D.V. Griffiths,[1] and M.D. Denavit[2]
[1] *Colorado School of Mines (email: d.v.griffiths@mines.edu)*
[2] *University of Illinois at Urbana-Champaign (email: denavit2@uiuc.edu)*

Abstract: Analysis of landslides starts with a reconsideration of the classical equations that govern "infinite slope" stability. In this paper two novel approaches for interpreting these equations are presented. First we look at probabilistic implications for infinite slope failure by implementing the First Order Reliability Method (FORM). This method is useful for assessing the sensitivity of the factor of safety to the various input parameters in the equations. Second we present an elasto-plastic finite element model of an infinite slope which is validated against the equations. The numerical approach has great potential since it is the only feasible method of analysis for more complex soil/water conditions and geometry.

INTRODUCTION

This paper revisits the classical equations of infinite slope stability analysis in order to better understand the mechanics of failure and the influence on the Factor of Safety of the various input parameters relating to shear strength, geometry and water conditions. Two quite different approaches are presented. First a FORM analysis is presented which enables the "probability of failure" of an infinite slope to be estimated as opposed to the more traditional "factor of safety". Such an analysis involves inputting the mean and standard deviation of the various input parameters together with a "performance function" that gives the combination of those parameters that would cause failure. FORM delivers the most likely values of the input parameters to cause failure and the probability that they would occur. A by-product of FORM is a set of sensitivity factors, which give a measure of the "importance" of each of the input parameters to the overall risk assessment. This is useful for any further studies by indicating to the investigator which parameters should be focused on, possibly at the expense of other less important parameters. The sensitivity factors are also useful in design and practice by indicating where mitigation efforts might be concentrated in potentially unsafe slopes. For a review of some of the classical methods of probabilistic slope stability analysis, including FORM, the interested reader is referred to Nadim *et al.* (2005).

The second part of the paper describes some elasto-plastic finite element (FE) analyses of infinite slopes and validates the numerical solutions against the classical infinite slope equations. Once the FE framework has been properly developed, the model will then have great potential for investigating more complex geometries, groundwater conditions and soil property variability. Other factors that may be of interest in later studies include the role of suctions above the water table and infiltration rates due to heavy rainfall. The key point is that numerical methods, and specifically the FE approach, offer the only feasible approach for realistic modeling of complex geotechnical systems that no longer fit the assumptions made in the classical equations.

BRIEF REVIEW OF INFINITE SLOPE THEORY

The infinite slope problem is a special case of general slope stability analysis in which the slope geometry is particularly simple as shown in Figure 1. The key assumption is that the slope, being "long" relative to the depth of soil in the potential sliding mass, leads to a potential failure mechanism that is translational and parallel to the ground surface.

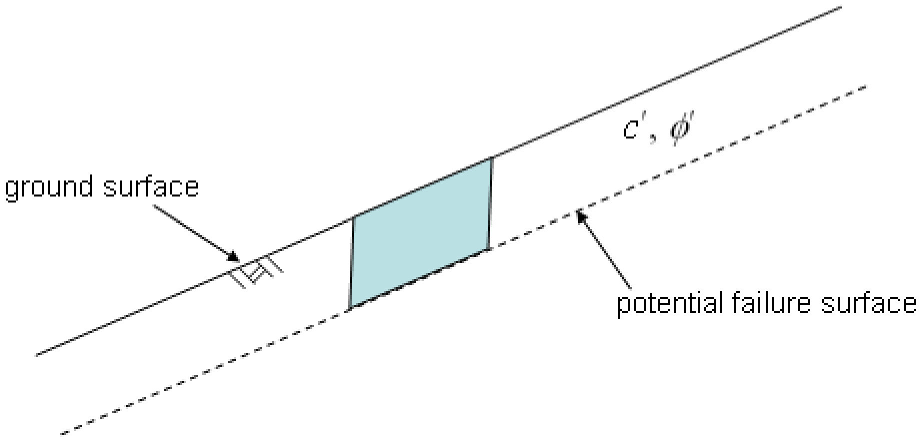

Figure 1. Infinite slope geometry.

Since the top and bottom of the slope are assumed to be so far away that they have no influence on the solution, we can consider the equilibrium of a typical slice anywhere within the potential sliding mass. Such a slice is shown in more detail in Figure 2 together with dimensions and the main forces acting on it.

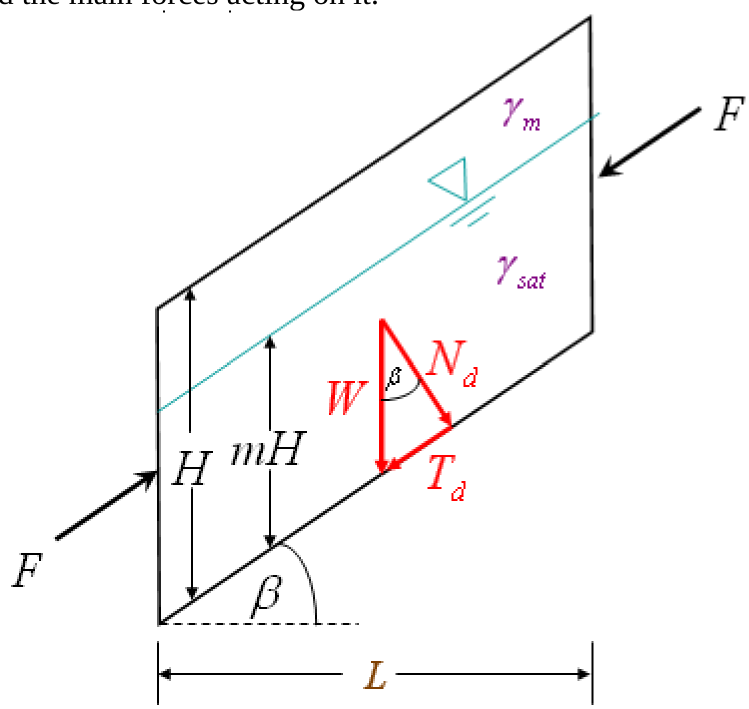

Figure 2. Geometry and forces acting on a typical slice of an infinite slope

The symbols on the figure and subsequent formulas are defined in Table 1.

Table 1. Notation used in infinite slope analysis

Symbol	Definition
$\phi' (\phi_u = 0)$	Drained friction angle (undrained friction angle)
$c' (c_u)$	Drained cohesion (undrained shear strength)
L	width of slice
H	soil depth
m	water table (WT) depth ratio
β	slope inclination
γ_m	moist or "dry" unit weight (above WT)
γ_{sat}	saturated unit weight (below WT)
γ'	buoyant unit weight ($\gamma_{sat} - \gamma_w$)
F	side forces
W	slice weight (total)
N_d	normal force (total)
T_d	developed shear force

If the maximum available shear resistance along the potential sliding surface is given by T_f, then the factor of safety can be defined:

$$FS = \frac{T_f}{T_d} \tag{1}$$

To account for the water table, we may assume the streamlines and equipotentials run, respectively, parallel and perpendicular to the ground surface leading to the following expression for the water pressure on the potential failure:

$$u = mH\gamma_w \cos^2 \beta \tag{2}$$

After some rearrangements, equation (1) can be written in its general form as:

$$FS = \frac{c'}{H(m\gamma_{sat} + (1-m)\gamma_m)\cos\beta \sin\beta} + \frac{m\gamma' + (1-m)\gamma_m}{m\gamma_{sat} + (1-m)\gamma_m} \frac{\tan\phi'}{\tan\beta} \tag{3}$$

A few useful special cases follow where for "dry" soil:

$$FS = \frac{c'}{H\gamma_m \cos\beta \sin\beta} + \frac{\tan\phi'}{\tan\beta} \tag{4}$$

for submerged soil:

$$FS = \frac{c'}{H\gamma_{sat}\cos\beta\sin\beta} + \frac{\gamma'}{\gamma_{sat}}\frac{\tan\phi'}{\tan\beta} \qquad (5)$$

and for "undrained clays" ($\phi_u = 0$):

$$FS = \frac{c_u}{H\gamma_{sat}\cos\beta\sin\beta} \qquad (6)$$

Some of equations (3)-(6) will form the basis of the analyses and validations described later.

REVIEW OF THE FIRST ORDER RELIABILITY METHOD (FORM)

Theory

The first order reliability method (FORM) is a process which can be used to determine the probability of a failure given the statistics (mean and standard deviation) of input data and a "limit state function". The method is based on the Hasofer-Lind reliability index (Hasofer and Lind 1974), β_{HL}, which can be described as the distance, in standard deviation units, between the most probable set of values and the most probable set of values that causes a failure. Calculation of this value is an iterative process, finding the minimum value of a matrix calculation subject to the constraint that the values result in a system failure. However, common solver routines found in several software packages (e.g. *Excel* and *Mathematica*) can easily arrive at the solution. Once the reliability index has been determined, the probability of failure, p_f, is a simple calculation.

Limit State Function

Each reliability analysis requires a limit state function, which defines failure or safe performance. Limit states could relate to strength failure, serviceability failure, or anything else that describes unsatisfactory performance. The limit state function, *g*, is defined

$$\begin{aligned} g(x_1,...,x_N) \geq 0 &\longrightarrow \text{Safe} \\ g(x_1,...,x_N) < 0 &\longrightarrow \text{Failure} \end{aligned} \qquad (7)$$

where N is the number of input random variables. Often it is sufficient for the limit state function to be the resistance minus the load. Other common forms of the limit state function are the factor of safety minus one and the logarithm of the factor of safety.

For relatively simple systems, the limit state function may be determined analytically, although for more complex systems it may need to be approximated numerically with curve fitting.

Hasofer-Lind Reliability Index

The reliability index, β_{HL}, is the distance in standard deviation units between the most probable set of random variables (the means), and the most probable set of random variables that causes a failure. Determination of β_{HL} is an iterative process and it is defined by:

$$\beta_{HL} = \min_{g=0} \sqrt{\left\{\frac{x_i - \mu_i}{\sigma_i}\right\}^T [R]^{-1} \left\{\frac{x_i - \mu_i}{\sigma_i}\right\}} \qquad i = 1, \ldots, N \tag{8}$$

where $\{(x_i-\mu_i)/\sigma_i\}$ is the vector of the random variable values reduced to standard normal space and $[R]$ is the correlation matrix of the variables.

Visualization

To better understand and visualize this method, consider the following arbitrary problem with *two* correlated random variables, x_1 and x_2, assumed to be normally distributed with the following parameters:

$$\begin{aligned} &\mu_{x_1} = 6.0 \quad \sigma_{x_1} = 1.0 \\ &\mu_{x_2} = 7.0 \quad \sigma_{x_2} = 0.75 \qquad \rho_{x_1,x_2} = -0.35 \end{aligned} \tag{9}$$

Let failure of the system be given by the limit state function:

$$g(x_1, x_2) = -0.03x_1^3 - 0.25x_2^2 + 29.16 = 0 \tag{10}$$

The probability density function governing two normal random variables correlated by ρ can be written as (e.g., Fenton and Griffiths 2007):

$$f_{x_1x_2}(x_1, x_2) = \frac{1}{2\pi\sigma_{x_1}\sigma_{x_2}\sqrt{1-\rho^2}} e^{\frac{-\beta(x_1,x_2)^2}{2}} \tag{11}$$

where

$$\beta(x_1, x_2) = \sqrt{\left\{\frac{x_i - \mu_{x_i}}{\sigma_{x_i}}\right\}^T [R]^{-1} \left\{\frac{x_i - \mu_{x_i}}{\sigma_{x_i}}\right\}} \qquad i = 1, 2 \tag{12}$$

Note that the minimum value of $\beta(x_1, x_2)$, given that the limit state function is zero, is the Hasofer-Lind reliability index, β_{HL}. Plotting the probability density function in three dimensions would result in a surface in the shape of a bell. By definition, the volume under the surface is unity. The limit state function divides the volume into a failure region and a safe region. The probability of failure is defined as the volume under the probability density function in the failure region. FORM uses a first order approximation of the limit state function and therefore the calculated probability of failure is also approximate. Numerical integration of the probability distribution function in the failure region leads to more accurate results and is discussed later.

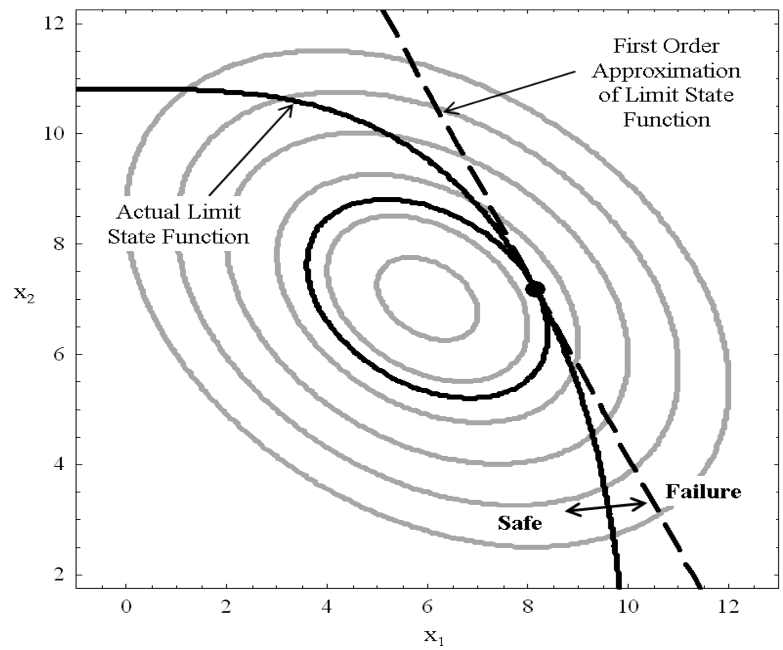

Figure 3. Plan view of the probability density function and the actual and approximated limit state functions

In plan view as shown in Figure 3, the probability density function can be visualized as a contour plot involving a series of ellipses, and the limit state function can be seen as a line separating the failure and safe regions. The contours in Figure 3 are actually contours of $\beta(x_1,x_2)$ (i.e. $\beta(x_1,x_2)$ = 1, 2, 3, 4…), nevertheless, each contour represents a constant value of the probability density function.

The solid curved line represents the actual limit state function. The smallest ellipse that the limit state function touches is the contour of $\beta = \beta_{HL}$, represented above by the darker ellipse. The point where they meet represents the most probable failure point. The dashed straight line that also passes through that point is the first order approximation of the limit state function.

The first order approximation assumed in FORM could lead to an underestimate of the probability of failure if the actual limit state function curves towards the mean values as seen in Figure 3. A more accurate, yet more time consuming, method to determine the probability is to numerically integrate the probability distribution function in the region of failure. A relatively simple algorithm involving the repeated mid-point rule (e.g., Griffiths and Smith 2006) can be devised to accomplish this task.

FORM software

Excel

The limit state function and properties described in equations (9) and (10) have been run through an Excel spreadsheet using the solver add-in (e.g., Low and Tang 1997, Xu and Low 2006, Denavit 2006) in which the FORM algorithm has been implemented. The Hasofer-Lind reliability index is given as $\beta_{HL\ L}$ = 2.40, corresponding to a probability of failure given by $p_f = 0.814\%$.

Mathematica

Using Mathematica, the same calculations can be performed. The following shows the lines which must be executed:

```
μx1 = 6.0; σx1 = 1.0; μx2 = 7.0; σx2 = 0.75; ρ = -0.35;
g[x1_, x2_] = -0.03 x1^3 - 0.25 x2^2 + 29.16;
Z1[x1_] = (x1 - μx1) / σx1; Z2[x2_] = (x2 - μx2) / σx2;
Z[x1_, x2_] = {Z1[x1], Z2[x2]}; R = {{1, ρ}, {ρ, 1}};
β[x1_, x2_] = √(Z[x1, x2].Inverse[R].Z[x1, x2]);
sol = Minimize[β[x1, x2], g[x1, x2] == 0, {x1, x2}]
{2.40244, {x1 → 8.1466, x2 → 7.19444}}
βHL = sol[[1]]; Dx1 = x1 /. sol[[2]]; Dx2 = x2 /. sol[[2]];
PfFORM = 1 - CDF[NormalDistribution[0, 1], βHL]
0.00814306
```

Again, the probability of failure is 0.814%, with a reliability index of 2.40, corresponding to a most probable failure point of x_1 = 8.15 and x_2 = 7.19. Both the reliability index and the most probable failure point can be graphically checked using Figure 1.

As discussed earlier, numerical integration can determine the probability of failure directly but more slowly. Below is a set of commands which will perform the numerical integration:

```
nsize = 8; ndivs = 1000; PfNInt = 0;
x1min = μx1 - nsize σx1; x1max = μx1 + nsize σx1;
x2min = μx2 - nsize σx2; x2max = μx2 + nsize σx2;
width = {(x1max - x1min) / ndivs, (x2max - x2min) / ndivs};
Area = width[[1]] * width[[2]];
means = {μx1, μx2}; cov = {{σx1^2, ρ σx1 σx2}, {ρ σx1 σx2, σx2^2}};
dist = MultinormalDistribution[means, cov];
For[i = 0, i < ndivs, i++, For[j = 0, j < numdivs, j++,
    value = {x1min + width[[1]] * (i + 0.5), x2min + width[[2]] * (j + 0.5)};
    If[g[value[[1]], value[[2]]] < 0, PfNInt = PfNInt + PDF[dist, value] * Area,]
   ];];
PfNInt
0.00963503
```

Numerical integration of the volume of the probability density function corresponding to $g(x_1, x_2) < 0$ gave the probability of failure 0.964% which is 16% higher than given by FORM.

PROBABILISTIC INFINITE SLOPE ANALYSIS

Infinite slope stability analysis is ideally suited to treatment by FORM since there are ready-made analytical solutions for FS as described earlier to operate on.

Starting with equation (3) and noting that failure of the slope corresponds to $FS = 1$, we can write a limit state function as:

$$g(c', \tan\phi', \gamma_{sat}, \gamma_m, m, \beta, H) = FS - 1 = 0 \quad (13)$$

where g is a function of up to seven random variables.

Consider an example problem with the following properties/dimensions which for this illustration will be assumed to be normally distributed as indicated in Table 2 (in each case a coefficient of variation of $V = \sigma/\mu = 0.3$ has been assumed).

A conventional calculation using equation (3) based on the mean values in Table 2 gives $FS = 1.45$ which would be considered an adequate factor of safety.

Table 2. Mean and standard deviation values used in example problem

	c' (kN/m^2)	$\tan\phi'$	γ_{sat} (kN/m^3)	γ_m(kN/m^3)	m	β	H (m)
μ	10	0.466	19	17.5	0.5	25°	2.0
σ	3	0.140	5.7	5.25	0.15	7.5	0.6

To demonstrate FORM, let us now treat the parameters in Table 2 as normally distributed uncorrelated random variables. Running these parameters, together with the limit state function given by equation (13) through FORM, leads to the most likely or "design" values of the seven parameters as shown in Table 3 to result in infinite slope failure.

Table 3. Most likely combination of parameters to cause infinite slope failure in the example problem

c' (kN/m^2)	$\tan\phi'$	γ_{sat} (kN/m^3)	γ_m(kN/m^3)	m	β	H (m)
8.69	0.400	19.70	18.02	0.52	30.6°	2.21

As a check, it is readily shown that if these parameters are substituted into equation (13) the result is $FS = 1$ $(g = 0)$. Comparing the design values from Table 3 to their mean values in Table 2 it is seen that both shear strength parameters are smaller than their mean values, but the other five parameters are all greater.

In addition to the design values shown in Table 3, FORM analysis gives an overall reliability index in this case of $\beta = 0.973$. Assuming a normal distribution, the reliability index is uniquely related to the probability of failure through the formula:

$$p_f = 1 - \Phi(\beta) \quad (14)$$

where $\Phi(\beta)$ is the standard normal cumulative distribution function (CDF). Standard tables then give us that:

$$\begin{aligned} p_f &= 1 - \Phi(0.973) \\ &= 0.165 \end{aligned} \tag{15}$$

A probability of failure of 0.165 or 16.5% is higher than might be anticipated for a slope with a "comfortable" factor of safety (based on the mean) as high as 1.45. What this emphasizes however is that the more uncertainty present in the input parameters of a system, the more vulnerable that system becomes to the formation of an "unlucky" combination of parameters resulting in failure.

It might be justifiably argued that most engineers would not use the mean values of highly variable soil properties in a conventional analysis. More likely they would use conservative values lower than the mean (see e.g. Griffiths and Fenton 2004) which would have led to a lower factor of safety. A final point to be considered here is that for the purposes of this demonstration exercise, a rather pessimistic assumption was made that all seven input parameters were random with the same coefficient of variation equal to 0.3. In a more realistic study, some of the parameters might be treated as random while others would be fixed to constant (or deterministic) values. In addition, the chosen random variables would unlikely have the same coefficients of variation. For example, unit weight is generally believed to have a much lower coefficient of variation than shear strength parameters say (see e.g. Lee *et al.* 1983).

A final by-product of a FORM analysis is the generation of "sensitivity parameters" summarized for this example in Table 4 in descending order.

Table 4. Sensitivity values for the seven parameters used in the FORM analysis

β	$\tan\phi'$	c'	H	m	γ_{sat}	γ_m
0.390	0.232	0.202	0.125	0.025	0.015	0.011

Sensitivity parameters give a guide to the relative importance of the random variables used in a FORM analysis. The sensitivity parameter of each variable is related to the slope of the limit state function with respect to that variable (e.g. $\partial g / \partial \beta$) at the design point. Sensitivity parameters for all the variables are normalized such that they sum to unity. In this case, the numbers in Table 4 indicate that the infinite slope analysis is most sensitive to the slope inclination (β) followed by the shear strength parameters $(\tan\phi'$ and $c')$ and the soil depth (H). The infinite slope stability analysis is shown to be least sensitive to the water depth (m) and the unit weights $(\gamma_{\mathrm{sat}}$ and $\gamma_{\mathrm{m}})$. Sensitivity information such as this enables engineers to decide which parameters may justify additional field or laboratory investment. The additional expense of such further testing may be offset by improved characterization of the problem and less conservative design.

REVIEW OF FINITE ELEMENT SLOPE STABILITY ANALYSIS

The elasto-plastic finite element method of slope stability has been amply described elsewhere (e.g. Griffiths and Lane 1999) so here we provide just a brief review.

The method involves setting up a finite element mesh covering the spatial extent of the slope problem under consideration. Knowing the unit weight of the soil in the slope, gravity loading is applied using a quite standard FE algorithm. The procedure then involves systematically reducing the shear strength of the soil using a gradually increasing strength reduction factor (SRF) as follows:

$$\phi'_F = \arctan\left(\frac{\tan\phi'}{SRF}\right) \quad \text{and} \quad c'_F = \frac{c'}{SRF} \tag{16}$$

where ϕ'_F and c'_F are the factored soil strength parameters being used in the analysis.

A point is eventually reached when the soil has been sufficiently weakened that it is no longer able to sustain the shear stresses generated by the gravity loading. At this point the displacements increase rapidly, the algorithm is unable to find a stress distribution that simultaneously satisfies global equilibrium and the Coulomb failure criterion and the factor of safety of the slope is given by:

$$FS \approx SRF \tag{17}$$

Application of FE to infinite slope analysis

Based on Program 6.3 in the text by Smith and Griffiths (2004) using 8-node plane-strain quadrilateral elements, a mesh generation routine was developed enabling analysis of a three-part slope problem of the type shown in Figure 4.

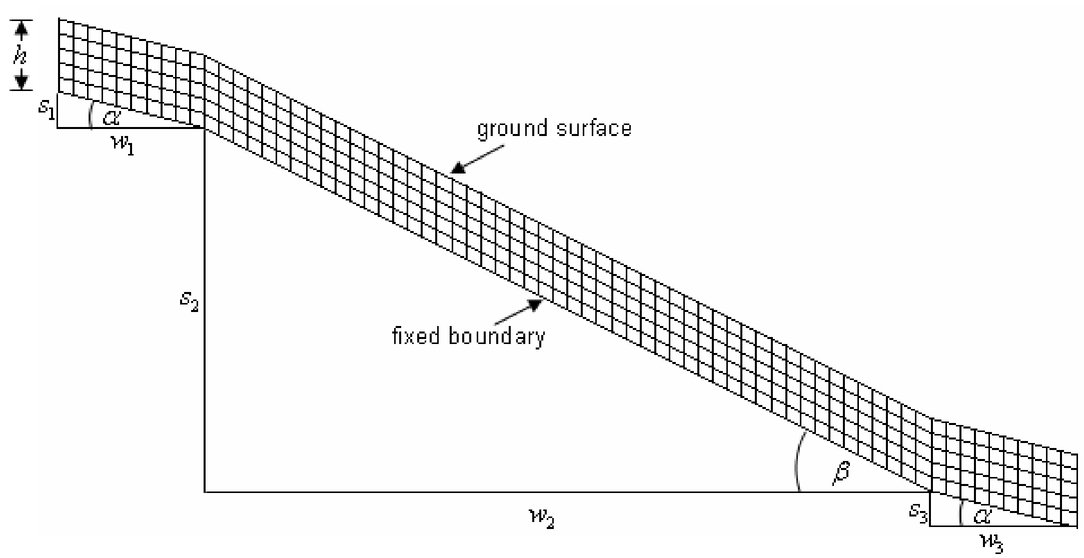

Figure 4. Typical three-stage mesh for analysis of long slopes

The user has control over the length and inclination of each section and the soil properties assigned to each element. The program also allows the thickness of the soil in each section to be varied, but only a constant h is considered here. A water table can also be implemented, not necessarily parallel to the main slope, but results including water pressures have not been included in this paper.

In setting up the model, various different boundary conditions were considered on the right and left vertical mesh boundaries in order to most closely reproduce results given by the "infinite slope" equations (3)-(6). Boundary conditions considered included various combinations of fixity involving rollers, "tied freedoms" and "skew boundary conditions". Some of these conditions involved quite customized modifications to the FE code and a detailed discussion of boundary conditions will be given more detailed treatment elsewhere. Only the simple case involving vertical roller boundary conditions to the left and right will be discussed here.

Validation of the FE program on an undrained clay slope

The first example is of an infinite slope of undrained clay $(\phi_u = 0)$ with the following properties and geometry:

$\phi_u = 0$
$c_u = 100$ kN/m^2
$H = 10$ m
$\gamma_{sat} = 20$ kN/m^3
$\beta = 26.6°$

These parameters substituted into equation (6) give:

$$FS = \frac{100}{10(20)\cos 26.6 \sin 26.6} = 1.25 \tag{18}$$

In the corresponding FE analysis, the central section was fixed to the required inclination with $\tan\beta = 0.5$ $(\beta = 26.6°)$ and the factor of safety FS computed for a range of gradients of the outer sections of the slope defined by $\tan\alpha$. The results plotted in Figure 5 give the factor of safety (FS) computed by FE vs. the "slope ratio" defined as $\tan\alpha/\tan\beta$. The factor of safety can be seen to be quite sensitive to the end slopes although good agreement with the classical solution of $FS = 1.25$ was obtained for $\tan\alpha/\tan\beta \approx 2$.

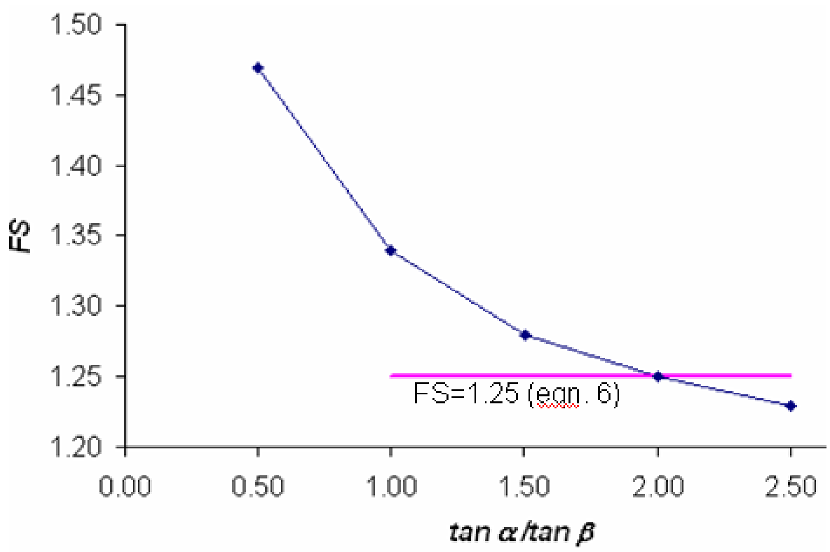

Figure 5. Influence of end slopes on *FS* for an undrained clay "infinite slope" analysis by FE

Figure 6 shows the deformed mesh at failure clearly demonstrating the concentrated zone of shear strain at the base of the mesh.

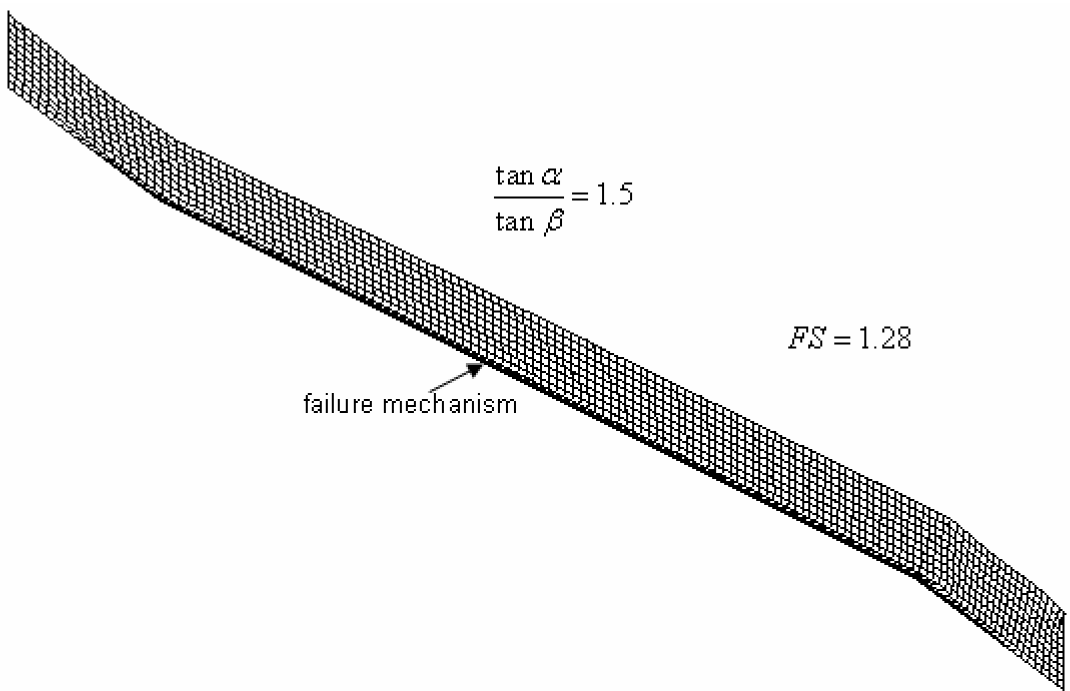

Figure 6. Deformed mesh at failure for undrained clay "infinite slope" analysis by FE

Validation of the FE program on a drained frictional slope

The second example is of an infinite slope of drained frictional soil with the following properties and geometry:

$\phi' = 15°$
$c' = 9.6$ kN/m^2
$H = 1.2$ m
$\gamma = 18.5$ kN/m^3
$\beta = 26.6°$

These parameters substituted into equation (4) give:

$$FS = \frac{9.6}{1.2(18.5)\cos 26.6 \sin 26.6} + \frac{\tan 15}{\tan 26.6} = 1.62 \qquad (19)$$

The results plotted in Figure 7 once more show FS vs. $\tan\alpha/\tan\beta$ for the frictional soil analysis.

In this case good agreement with the classical solution of $FS = 1.62$, was obtained closer to $\tan\alpha/\tan\beta \approx 1.5$.

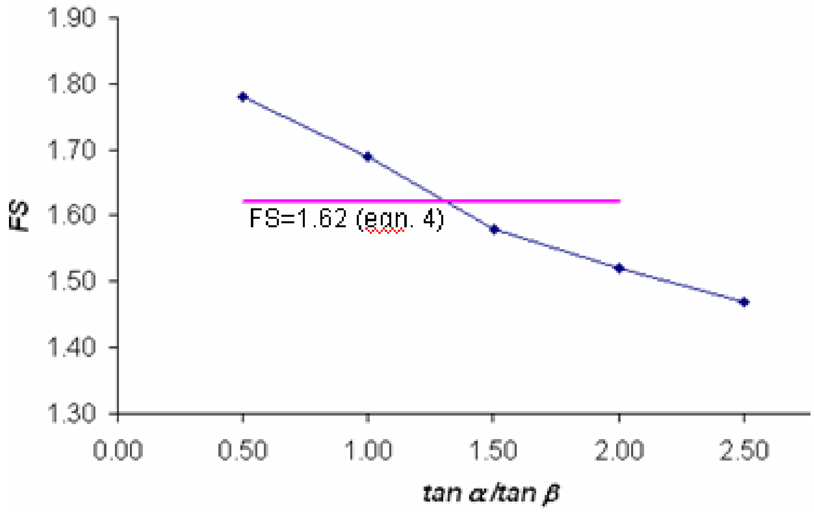

Figure 7. Influence of end slopes on *FS* for frictional soil "infinite slope" analysis by FE

Note on "tied freedoms"

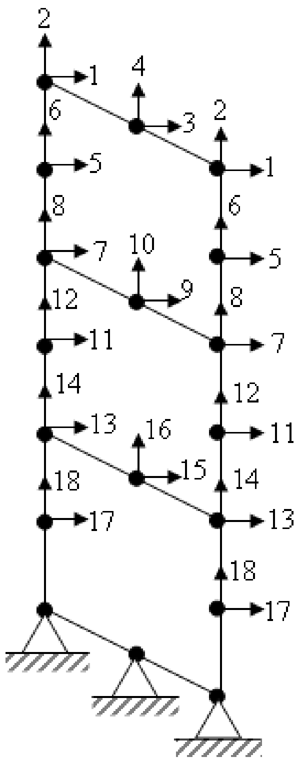

Figure 8. Freedom numbering for "infinite slope" analysis by FE with "tied freedoms"

The FE models have been validated rather successfully against classical solutions, however they did require a high number of elements and a significant lateral extent to avoid interference from the boundaries. Recent work has concentrated on a much less computationally intensive model involving a single column of elements and "tied freedoms" as indicated in the schematic in Figure 8.

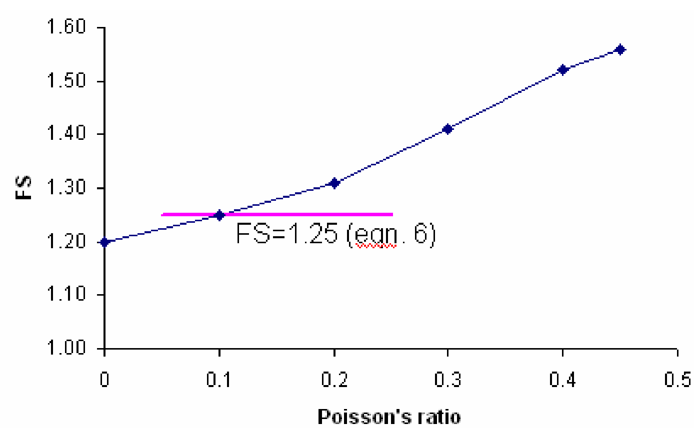

Figure 9. *FS* vs. Poisson's ratio for an undrained clay "infinite slope" analysis by FE using "tied freedoms".

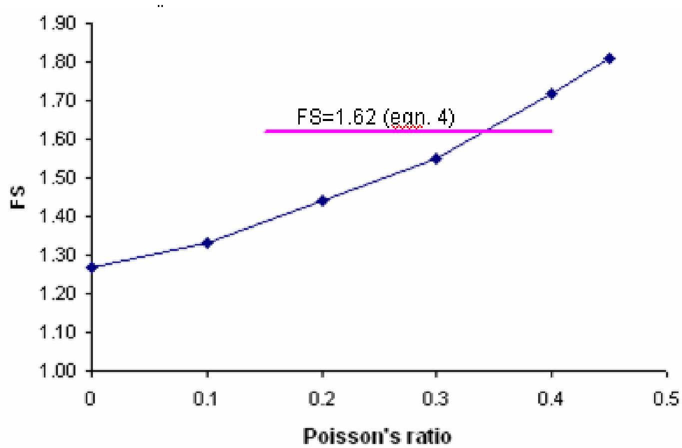

Figure 10. *FS* vs. Poisson's ratio for a frictional soil "infinite slope" analysis by FE using "tied freedoms".

The idea of tied freedoms in this context is to force the left and right sides of the column to move identically by mimicking the "infinite slope" assumption in which there is no bias to either side of a typical column. Initial analyses using this model are encouraging, but need further work since the rather confined nature of the enforced deformations has introduced a "Poisson's ratio effect" as shown in the results given in Figures 9 and 10 for the same problems considered previously. Clearly the factor of safety increases quite significantly with Poisson's ratio.

Figures 11(a) and (b) show, respectively, the deformed mesh and displacement vectors at failure using tied freedoms. It may be observed for example, that the nodal displacement vector at the top left corner is identical to the displacement vector at the top right and so on.

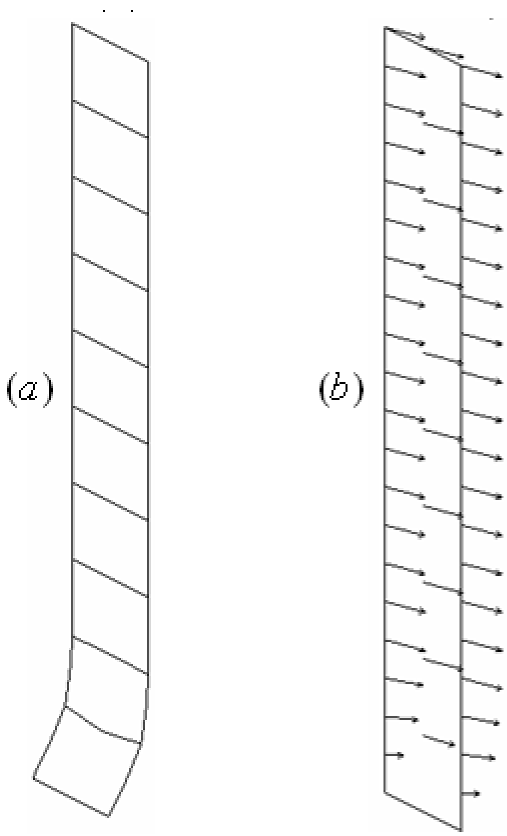

Figure 11. Deformed mesh (a) and nodal displacement vectors (b) at failure for an undrained clay “infinite slope” analysis by FE using “tied freedoms”.

CONCLUDING REMARKS

The paper has introduced two methods of analysis of landslides via the classical “infinite slope” equations. The first approach used the first order reliability method (FORM) to predict the probability of infinite slope failure in terms of up to seven random input variables. Although the method does not properly account for spatial correlation effects, it is able to give qualitative estimates of the sensitivity of the infinite slope stability problem to the various input parameters. In the example presented here, the “most important” parameters appeared to be the slope angle β and the shear strength parameters $\tan\phi'$ and c' while the unit weights γ_{sat} and γ_m appeared least important. A spreadsheet program using the FORM methodology has been developed and will form the basis of future research on this subject.

The second approach involved adapting an existing elasto-plastic finite element slope stability program. Although the infinite slope geometry is rather simple, the incorporation of appropriate boundary conditions to reproduce an “infinite” condition provided an initial challenge. A simple approach was to extend the mesh laterally a sufficient distance such that the side boundary conditions became unimportant. Good agreement with the classical equations was obtained by adjusting the gradient of the side slopes. This method was rather computationally intensive however due to the large number of elements required, so a second approach is currently under development involving the use of “tied freedoms” allowing analysis of a single column of elements. Initial results are encouraging, however the confined nature of the enforced displacements introduced a Poisson's ratio effect which needs further investigation.

Numerical modeling via the finite element method offers one of the most powerful tools for analyzing landslide phenomena. An effective and properly validated finite element framework will have great potential for improved understanding of the mechanics and mitigation of landslides. In combination with probabilistic tools such as FORM in order to assess sensitivities, future FE research will be able to investigate influences such as spatially varying soil properties, ground water flow conditions, slope geometry, pore water suctions and infiltration.

Acknowledgements: The authors wish to acknowledge the support of NSF grant CMS-0408150 on "Advanced probabilistic analysis of stability problems in geotechnical engineering".

Corresponding author: D.V. Griffiths, Ph.D., P.E., F.ASCE, Geomechanics Research Center, Division of Engineering, Colorado School of Mines, Golden, Colorado 80401-1887, United States of America; Email: d.v.griffiths@mines.edu

REFERENCES

DENAVIT, M.D. 2006. *Probabilistic Geotechnics*, Independent Study Report, Colorado School of Mines, Golden, Colorado.

FENTON, G.A., and GRIFFITHS, D.V. 2007. *Risk assessment in geotechnical engineering*, John Wiley & Sons, Hoboken, NJ, Under contract.

GRIFFITHS, D.V. and FENTON, G.A. 2004. Probabilistic slope stability analysis by finite elements, *J Geotech Geoenv Eng*, **130**(3), 507-518.

GRIFFITHS, D.V., and LANE, P.A. 1999. Slope stability analysis by finite elements. *Géotechnique*, **49**(3), 387-403.

GRIFFITHS, D.V., and SMITH, I.M. 2006. *Numerical Methods for Engineers (2nd ed.)*, CRC Press, Boca Raton, FL

HASOFER, A.M., and LIND, N.C. 1974. Exact and invariant second-moment code format. *Journal of Engineering Mechanics*, ASCE, **100**, 111-121.

LEE, I.K., WHITE, W. and INGLES, O.G. 1983. *Geotechnical Engineering*, Pitman, London.

NADIM, F., EINSTEIN, H. and ROBERDS, W. 2005. State of Art 3 -Probabilistic stability analysis for individual slopes in soil and rock. International Conference on Landslide Risk Management, Vancouver, Canada, 31 May-2 June 2005.

LOW, B.K., and TANG, W.H. 1997. Efficient reliability evaluation using spreadsheet. *Journal of Engineering Mechanics*, ASCE, **123**(7), 749-752.

SMITH, I.M. and GRIFFITHS, D.V. 2004. *Programming the finite element method (4th ed)*), John Wiley & Sons, Chichester.

XU, B. and LOW, B. K. 2006. Probabilistic stability analyses of embankments based on finite-element method, *Journal of Geotechnical and Geoenvironmental Engineering*, ASCE, Vol. 132, No. 11, pp 1444-1454,